

Full Paper

Complete Disruption of All Nitric Oxide Synthase Genes Causes Markedly Accelerated Renal Lesion Formation Following Unilateral Ureteral Obstruction in Mice In Vivo

Naoya Morisada¹, Masayoshi Nomura², Hisae Nishii², Yumi Furuno³, Mayuko Sakanashi⁴, Ken Sabanai³, Yumiko Toyohira³, Susumu Ueno³, Seiji Watanabe¹, Masahito Tamura⁵, Tetsuro Matsumoto², Akihide Tanimoto⁶, Yasuyuki Sasaguri⁷, Hiroaki Shimokawa⁸, Koichi Kusuhara¹, Nobuyuki Yanagihara³, Akira Shirahata¹, and Masato Tsutsui^{3,4,*}

Departments of¹Pediatrics, ²Urology, ³Pharmacology, ⁵Internal Medicine, and ⁷Pathology, School of Medicine, University of Occupational and Environmental Health, Kitakyushu 807-8555, Japan

⁴Department of Pharmacology, Graduate School of Medicine, University of the Ryukyus, Okinawa 903-0215, Japan

⁶Department of Pathology, Kagoshima University Graduate School of Medical and Dental Sciences, Kagoshima 890-8544, Japan

⁸Department of Cardiovascular Medicine, Tohoku University Graduate School of Medicine, Sendai 980-8574, Japan

Received May 20, 2010; Accepted September 27, 2010

Abstract. The role of nitric oxide (NO) derived from all three NO synthases (NOSs) in renal lesion formation remains to be fully elucidated. We addressed this point in mice lacking all NOSs. Renal injury was induced by unilateral ureteral obstruction (UUO). UUO caused significant renal lesion formation (tubular apoptosis, interstitial fibrosis, and glomerulosclerosis) in wild-type, singly, and triply NOS^{-/-} mice. However, the extents of renal lesion formation were markedly and most accelerated in the triply NOS^{-/-} genotype. UUO also elicited the infiltration of inflammatory macrophages, up-regulation of transforming growth factor (TGF)- β 1, and induction of epithelial mesenchymal transition (EMT) in all of the genotypes; however, the extents were again largest by far in the triply NOS^{-/-} genotype. Importantly, long-term treatment with the angiotensin II type 1 (AT₁)-receptor blocker olmesartan significantly prevented the exacerbation of those renal structural changes after UUO in the triply NOS^{-/-} genotype, along with amelioration of the macrophage infiltration, TGF- β 1 levels, and EMT. These results provide the first evidence that the complete disruption of all NOS genes results in markedly accelerated renal lesion formation in response to UUO in mice in vivo through the AT₁-receptor pathway, demonstrating the critical renoprotective role of all NOSs-derived NO against pathological renal remodeling.

Keywords: nitric oxide synthase, renal remodeling, unilateral ureteral obstruction, knockout mouse, angiotensin

Introduction

Nitric oxide (NO) plays an important role in maintaining renal homeostasis (1 – 3). Endogenous NO is formed from its precursor L-arginine by a family of NO synthases (NOSs) with stoichiometric production of L-citrulline (4 – 10). Three distinct NOS isoforms exist: neuronal

(nNOS or NOS1), inducible (iNOS or NOS2), and endothelial NOS (eNOS or NOS3). All NOS isoforms are expressed in the kidney in both physiological and pathological situations.

Chronic unilateral ureteral obstruction (UUO) is a well-characterized model of experimental obstructive nephropathy, culminating in renal tubular apoptosis, interstitial fibrosis, and glomerulosclerosis (11, 12). These alterations are also a common feature associated with a variety of kidney disorders, including chronic kidney disease (CKD) and end-stage renal disease (ESRD) (13).

*Corresponding author (affiliation #4). tsutsui@med.u-ryukyuu.ac.jp
Published online in J-STAGE on November 9, 2010 (in advance)
doi: 10.1254/jphs.10143FP

It has been reported that eNOS plays a role in suppressing renal interstitial fibrosis after UUO in a study with eNOS-deficient (eNOS^{-/-}) mice (14), and that iNOS plays a role in attenuating renal tubular apoptosis (11) and interstitial fibrosis (15, 16) following UUO in studies with iNOS^{-/-} mice. On the other hand, the role of NO derived from all NOSs in the UUO model has been examined in pharmacological studies with non-selective NOS inhibitors such as L-arginine methyl ester (L-NAME). However, the results of the studies with L-NAME are conflicting: intraperitoneal treatment with L-NAME for 7 days significantly increased renal tubular apoptosis of the mouse obstructed kidney after UUO (11), whereas oral treatment with L-NAME in drinking water for 6 days did not significantly affect renal interstitial fibrosis of the rat obstructed kidney after UUO (12). Thus, the precise role of NO derived from all NOSs in renal remodeling still remains to be fully elucidated. To address this point, in this study we used mice that lack all three NOS genes (triple n/i/eNOS^{-/-} mice) (17, 18).

Although multiple mechanisms contribute to the progression of renal injury induced by UUO, a potential role of the renin-angiotensin system has been suggested. Angiotensin II contents in the kidney were significantly increased in rats with UUO (19). In these animals, gene expression of the angiotensin II type 1 (AT₁) receptor and the binding affinity of angiotensin II with the AT₁ receptor in the kidney were also increased (20). Treatment with the AT₁-receptor blockers (21) or angiotensin-converting enzyme (ACE) inhibitors (22) is known to ameliorate UUO-induced renal injury in mice and rats. Other studies have shown that UUO-induced renal fibrosis is reduced in mice lacking angiotensinogen (23) or the AT_{1a} receptor (24). On the basis of these findings, in this study we also investigated the effects of long-term treatment with the AT₁-receptor blocker olmesartan on the UUO-induced renal remodeling in the triple n/i/eNOS^{-/-} mice.

Materials and Methods

Animal preparation

This study was reviewed and approved by the Ethics Committee of Animal Care and Experimentation, University of Occupational and Environmental Health, Japan and University of the Ryukyus, Japan and was carried out according to the Institutional Guidelines for Animal Experimentation and the Law (No.105) and Notification (No.6) of the Japanese Government. This investigation conformed to the Guide for the Care and Use of Laboratory Animals published by the US National Institutes of Health (NIH Publication No. 85-23, revised 1996). Experiments were performed in 8–12-week-old male

wild-type (WT), singly nNOS^{-/-}, iNOS^{-/-}, eNOS^{-/-}, and triple n/i/eNOS^{-/-} mice. The genotypes for the nNOS, iNOS, and eNOS genes were determined by polymerase chain reaction (PCR) of tail genomic DNA (17). We generated the triple n/i/eNOS^{-/-} mice by crossing singly NOS^{-/-} mice, as previously reported (17). Systolic blood pressure was measured by the tail-cuff method under conscious conditions (Model MK-2000; Muromachi Kikai Co., Ltd., Tokyo).

UUO

Surgical procedures were performed under general anesthesia with pentobarbital (60 mg/kg, i.p.) (Kyoritsu Seiyaku Corporation, Tokyo). The abdomen was opened by a left lateral incision, and the left proximal ureter was exposed and permanently ligated with 3-0 nylon sutures. Sham-operated mice had their ureter exposed but not ligated. The incision was then closed with 3-0 silken threads. On days 3, 7, and 14 following UUO, the mice were euthanized by inhalation of an overdose of diethyl ether (Wako Pure Chemical Industries, Osaka), and the kidneys were harvested. The isolated kidneys were fixed in 10% phosphate-buffered formalin and embedded in paraffin for histological analysis. Portions of the kidneys were stored at -80°C, until ACE activity, transforming growth factor (TGF)- β 1, NOx (nitrite plus nitrate), or angiotensin II levels were assayed.

Histological analysis

Kidney slices 5- μ m-thick were stained with hematoxylin-eosin, Masson-Trichrome, or periodic acid-Schiff (PAS) solutions for evaluating tubular apoptosis, interstitial fibrosis, or glomerulosclerosis, respectively. The sections were scanned with a light microscope equipped with a 2-dimensional analysis system (Axiovert 135TV; Carl Zeiss, Jena, Germany) (25). The extent of tubular apoptosis was determined by counting the number of apoptotic and non-apoptotic cells, and expressed as the percentage of the apoptotic cell number per 100 cells studied. The extent of interstitial fibrosis was analyzed by using a standard point-counting method (26, 27) and expressed as the percentage of the fibrotic grid points to the total grid points examined. The extent of glomerulosclerosis was assessed by counting the number of glomeruli with and without global glomerular sclerosis and expressed as the percentage of the global sclerotic glomeruli number to the total glomeruli number evaluated. All the analyses were performed in a blind manner by two independent investigators (an experienced pathologist and a physician), and the mean values were used.

Immunostaining

Paraffin-embedded kidney sections were incubated

with a rat monoclonal F4/80 antibody (AbD Serotec, Raleigh, NC, USA), a rabbit polyclonal TGF- β 1 antibody (Santa Cruz Biotechnology, Santa Cruz, CA, USA), or a mouse monoclonal α -smooth muscle actin (SMA) (Dako, Tokyo) (28), as we previously reported (25). F4/80 is a 160-kDa plasma membrane component of mouse mononuclear phagocytes and a marker of macrophages (29). The number of F4/80-positive macrophages was counted in 10 consecutive non-overlapping high power fields (15). The α -SMA-positive area was analyzed by a standard point-counting method (26, 27).

TGF- β level

The expression levels of TGF- β 1 in the kidney were evaluated with a TGF- β 1 ELISA kit (Promega Corporation, Madison, WI, USA). The obtained values were corrected by wet tissue weight.

ACE activity

The renal ACE activity was measured with an ACE activity assay kit (Life laboratory, Yamagata), as we previously reported (30).

NOx level

NOx levels in the kidneys were assayed by the Griess method, as previously reported (31).

Angiotensin II level

The mice were sacrificed by cervical dislocation, and angiotensin II levels in isolated kidneys were analyzed with an angiotensin II EIA kit (Phoenix Pharmaceuticals, Inc., Burlingame, CA, USA).

Drug treatment

To examine the effects of pharmacological treatments on UUU-induced renal lesion formation, the following six groups were studied: untreated control WT and n/i/eNOS^{-/-} mice, WT and n/i/eNOS^{-/-} mice that received olmesartan (5 mg/kg per day, Daiichi Sankyo Co., Ltd., Tokyo) in chow (30), and WT and n/i/eNOS^{-/-} mice that received hydralazine (0.05 mg/ml; Sigma, St. Louis, MO, USA) in drinking water (30). In addition, to study the effects of NO supplementation, the following two groups were studied: untreated control n/i/eNOS^{-/-} mice and n/i/eNOS^{-/-} mice that received isosorbide dinitrate (ISDN, 0.3 mg/ml; Eisai Co., Ltd., Tokyo) in drinking water (32). These treatments were performed for 14 days, from 7 days before to 7 days after UUU.

Statistical analyses

Results are expressed as the mean \pm S.E.M. Statistical analysis was performed by ANOVA followed by Scheffe post-hoc test for multiple comparisons. A value of

$P < 0.05$ was considered to be statistically significant.

Results

Exacerbated renal architecture after UUU in mice lacking all NOSs

We first examined the time course of renal structural changes before and on days 3, 7, and 14 after UUU in the WT and triply n/i/eNOS^{-/-} mice (Fig. 1A). Before UUU, mild but significant renal tubular apoptosis (Fig. 1B) was seen in the triply n/i/eNOS^{-/-} mice as compared with the WT mice, as we previously reported (17). In both the WT and triply n/i/eNOS^{-/-} mice, UUU caused significant increases in renal tubular dilatation (Fig. 1A), tubular apoptosis (Fig. 1B), interstitial fibrosis (Fig. 1C), and global glomerulosclerosis (Fig. 1D). However, the extents of those UUU-induced renal structural changes were markedly larger in the triply n/i/eNOS^{-/-} than in the WT mice (Fig. 1).

We next compared the extents of the UUU-induced renal lesion formation among the WT, singly NOS^{-/-}, and triply NOS^{-/-} mice. Because significant differences in renal tubular apoptosis in the WT and triply n/i/eNOS^{-/-} mice were noted on days 3 and 7, but not on day 14, after UUU (Fig. 1B), the following experiments were performed on day 7 after UUU (Fig. 2A). While renal tubular apoptosis on day 7 after UUU was significantly enhanced in the singly iNOS^{-/-} and triply n/i/eNOS^{-/-} mice as compared with the WT mice, its extent was largest in the triply n/i/eNOS^{-/-} mice (Fig. 2B). While interstitial fibrosis on day 7 after UUU was augmented in the singly iNOS^{-/-}, eNOS^{-/-}, and triply n/i/eNOS^{-/-} mice compared with the WT mice, its extent was also greatest in the triply n/i/eNOS^{-/-} mice (Fig. 2C). Furthermore, while global glomerulosclerosis on day 7 after UUU was significantly increased in the singly eNOS^{-/-} and triply n/i/eNOS^{-/-} mice, it was again most accelerated in the triply n/i/eNOS^{-/-} mice (Fig. 2D).

Increased renal macrophage infiltration after UUU in mice lacking all NOSs

We then investigated the involvement of inflammation by evaluating the infiltration of F4/80-immunoreactive macrophages. UUU significantly increased the number of renal F4/80-positive macrophages in all the WT, singly NOS^{-/-}, and triply NOS^{-/-} strains studied (Fig. 3: A, B). When compared with the WT mice, the number of renal F4/80-positive macrophages on day 7 after UUU was significantly larger only in the triply n/i/eNOS^{-/-} mice, but not in any singly NOS^{-/-} mice (Fig. 3: A, B).

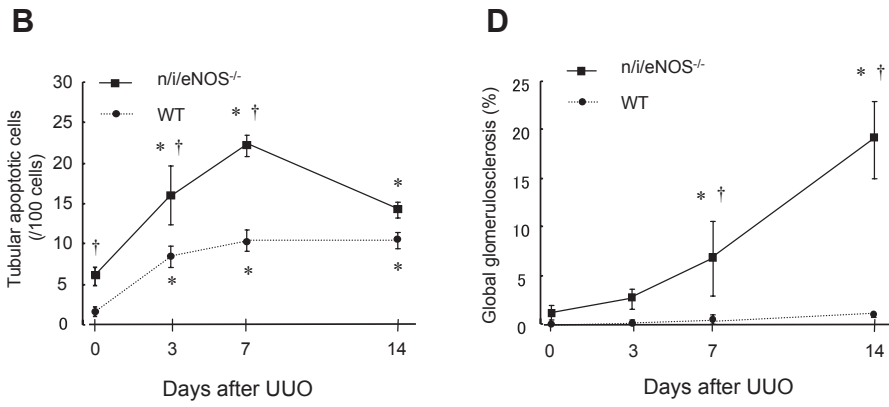
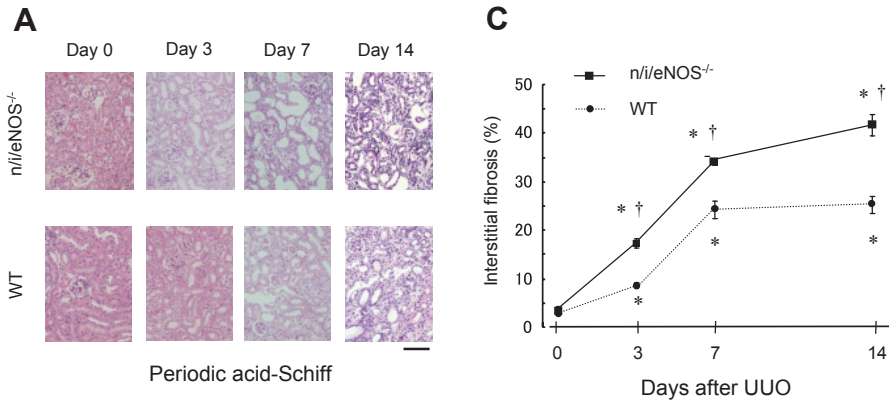


Fig. 1. Renal lesions before and on days 3, 7, and 14 after unilateral ureteral obstruction (UUO) in wild-type (WT) and triply n/i/eNOS^{-/-} mice. **A:** Periodic acid-Schiff (PAS) staining in the obstructed kidney of the WT and n/i/eNOS^{-/-} mice before and on days 3, 7, and 14 after UUO. The scale bar indicates 100 μm. **B:** The number of renal tubular apoptotic cells (n = 4–7). **C:** Renal interstitial fibrosis (n = 6–10). **D:** Global glomerulosclerosis (n = 4–7). *P < 0.05 vs. Day 0, †P < 0.05 vs. WT.

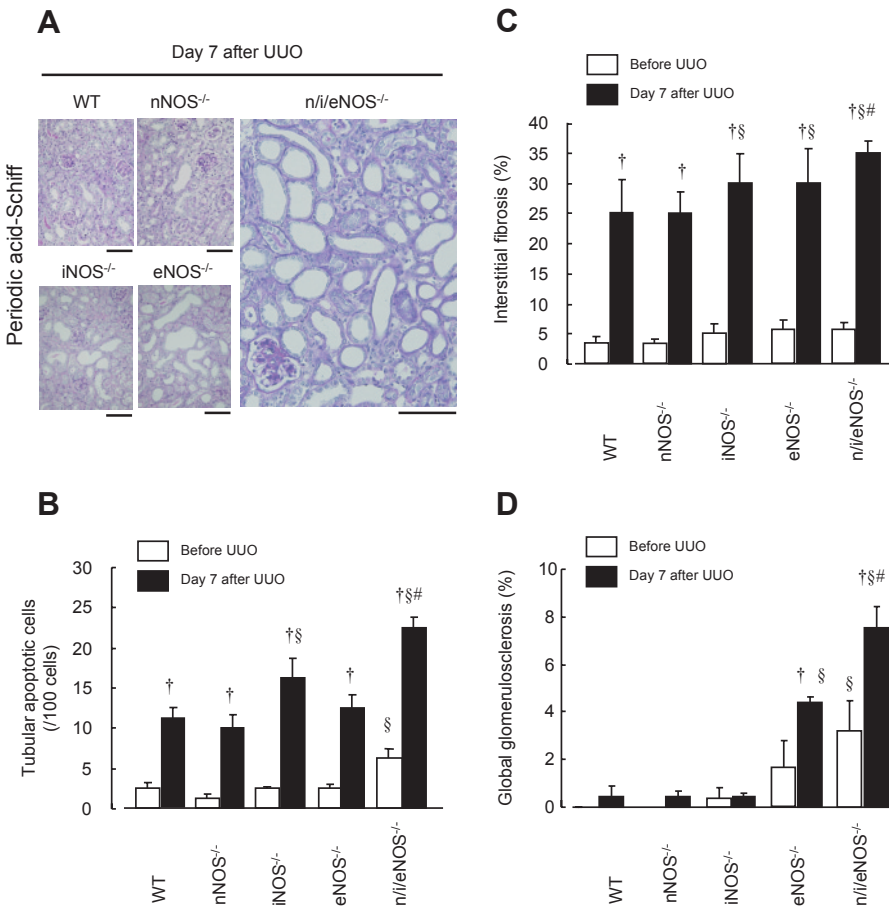


Fig. 2. Renal lesions before and on day 7 after UUO in WT, singly, and triply NOS^{-/-} mice. **A:** PAS staining in the obstructed kidney. Scale bars show 100 μm. **B:** The number of renal tubular apoptotic cells (n = 4–5). **C:** Renal interstitial fibrosis (n = 6–10). **D:** Global glomerulosclerosis (n = 4–5). †P < 0.05 vs. before UUO, §P < 0.05 vs. WT, #P < 0.05 vs. iNOS^{-/-} or eNOS^{-/-}.

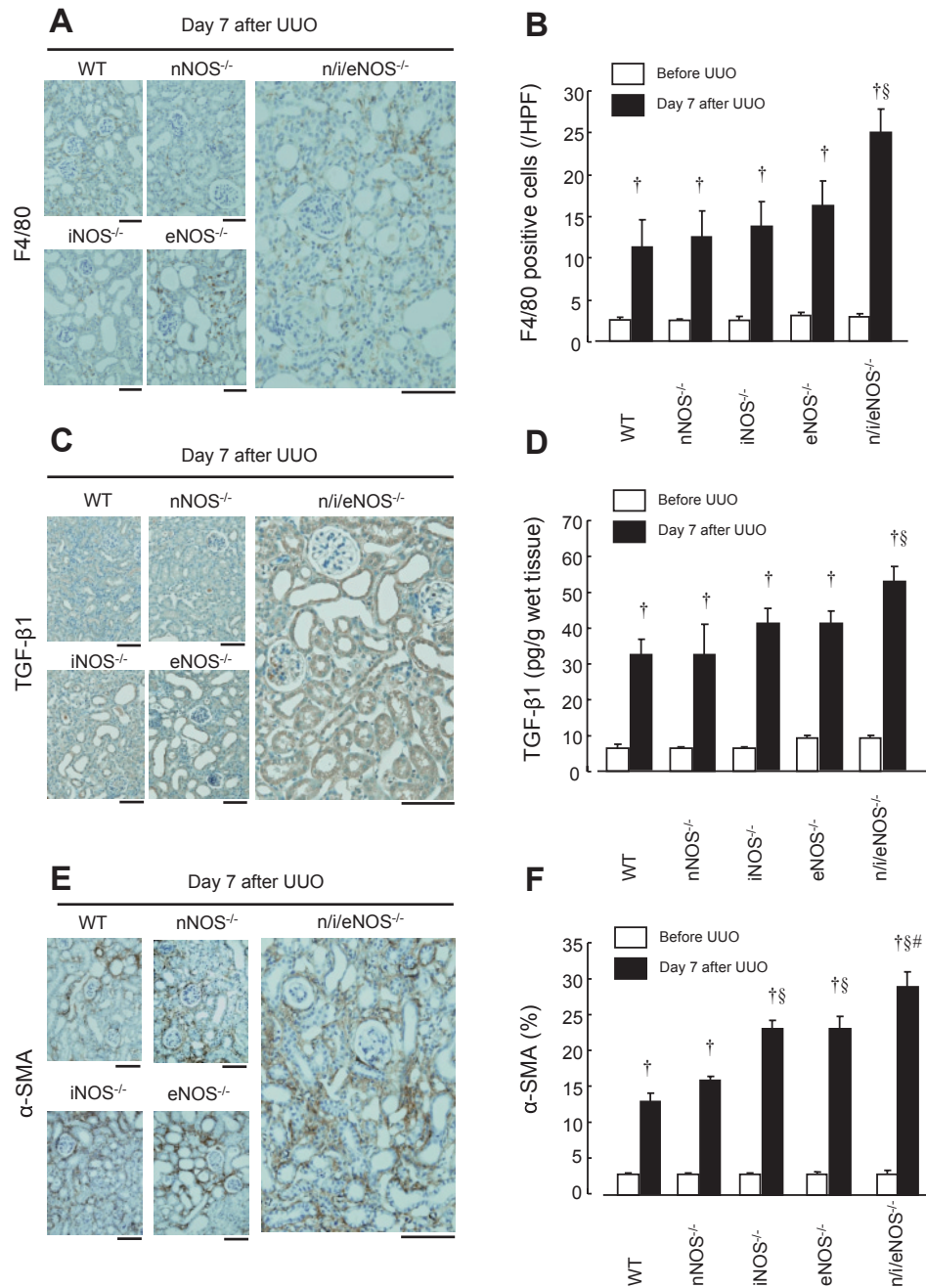


Fig. 3. F4/80-immunoreactive macrophages, transforming growth factor (TGF)- β 1, and α -smooth muscle actin (α -SMA) levels before and on day 7 after UUO in WT, singly NOS^{-/-}, and triply NOS^{-/-} mice. Scale bars in panels A, C, and E represent 100 μ m. A: Immunostaining for F4/80, a marker of macrophages, on day 7 after UUO in the obstructed kidney. B: The number of F4/80-positive cells per high power field (HPF) in the obstructed kidney (n = 4–5). C: Immunostaining for TGF- β 1 on day 7 after UUO in the obstructed kidney. D: TGF- β 1 protein levels of the obstructed kidney measured by ELISA (each, n = 5). E: Immunostaining for α -SMA on day 7 after UUO in the obstructed kidney. F: α -SMA-immunoreactive area in the obstructed kidney (n = 4–6). [†]P < 0.05 vs. before UUO, [§]P < 0.05 vs. WT, [#]P < 0.05 vs. iNOS^{-/-} or eNOS^{-/-}.

Enhanced renal TGF- β 1 levels after UUO in mice lacking all NOSs

TGF- β 1 is implicated in renal pathology, including interstitial fibrosis. Both immunostaining and ELISA for TGF- β 1 revealed that UUO significantly up-regulated

renal TGF- β 1 protein levels in all the WT, singly NOS^{-/-}, and triply NOS^{-/-} genotypes (Fig. 3: C, D). The renal TGF- β 1 levels on day 7 after UUO were significantly higher only in the triply n/i/eNOS^{-/-} mice, but not in any singly NOS^{-/-} mice, as compared with the WT mice (Fig.

3: C, D). There was a significant correlation between the renal TGF- β 1 levels and the extent of renal interstitial fibrosis on day 7 after UUO ($r = 0.993$, $n = 9$, $P < 0.05$).

Augmented renal α -SMA levels after UUO in mice lacking all NOSs

We studied the involvement of epithelial mesenchymal transition (EMT) by assessing the immunoreactivity of α -SMA, which is a marker of mesenchymal myofibroblasts. UUO significantly increased the renal α -SMA-positive area in all the WT, singly $\text{NOS}^{-/-}$, and triply $\text{NOS}^{-/-}$ genotypes (Fig. 3: E, F). Although significant increases in the renal α -SMA-positive area on day 7 after UUO were found in the singly $\text{iNOS}^{-/-}$, $\text{eNOS}^{-/-}$, and triply $\text{n/i/eNOS}^{-/-}$ mice, the greatest increase was noted

in the triply $\text{n/i/eNOS}^{-/-}$ mice. There was a significant correlation between the renal α -SMA-positive area and the extent of renal interstitial fibrosis on day 7 after UUO ($r = 0.976$, $n = 9$, $P < 0.05$).

NO supplementation prevents renal lesion formation after UUO in mice lacking all NOSs

We examined whether NO supplementation by long-term treatment with the NO donor ISDN would prevent renal lesion formation after UUO in the $\text{n/i/eNOS}^{-/-}$ mice (Fig. 4A). Long-term treatment with ISDN for 14 days significantly attenuated the UUO-induced increases in renal tubular apoptosis (Fig. 4B), interstitial fibrosis (Fig. 4C), and global glomerulosclerosis (Fig. 4D) in the $\text{n/i/eNOS}^{-/-}$ mice. The long-term treatment with ISDN

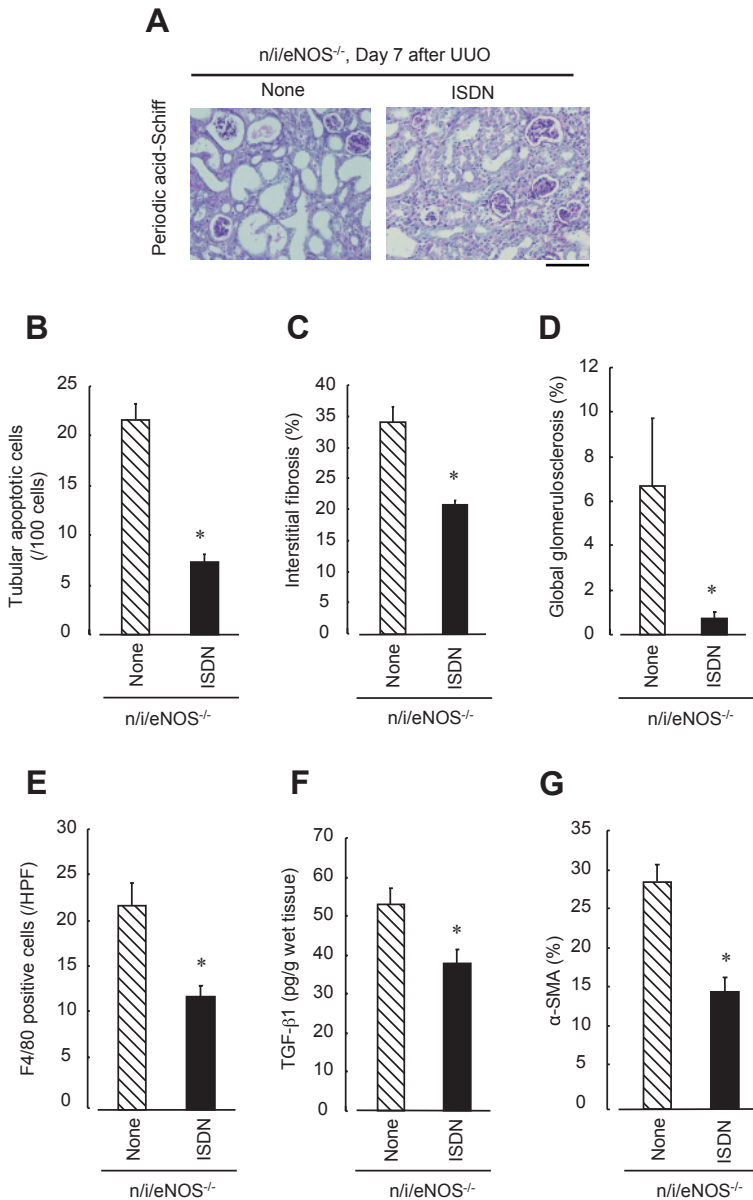


Fig. 4. Effects of long-term treatment with isosorbide dinitrate (ISDN) for 14 days in the $\text{n/i/eNOS}^{-/-}$ mice. **A:** PAS staining in the obstructed kidney of the $\text{n/i/eNOS}^{-/-}$ mice with and without the ISDN treatment on day 7 after UUO. The scale bar indicates 100 μm . **B:** The number of renal tubular apoptotic cells in the obstructed kidney of the $\text{n/i/eNOS}^{-/-}$ mice with and without the ISDN treatment on day 7 after UUO ($n = 4 - 5$). **C:** Interstitial fibrosis ($n = 8 - 10$). **D:** Global glomerulosclerosis ($n = 4 - 5$). **E:** The number of F4/80-positive cells ($n = 4 - 5$). **F:** TGF- β 1 protein levels (each, $n = 5$). **G:** α -SMA-immunoreactive area ($n = 4 - 5$). * $P < 0.05$ vs. none.

also suppressed the UUU-induced increases in the number of renal F4/80-positive macrophages (Fig. 4E), the

TGF- β 1 levels (Fig. 4F), and the α -SMA-positive area (Fig. 4G) in the n/i/eNOS $^{-/-}$ mice.

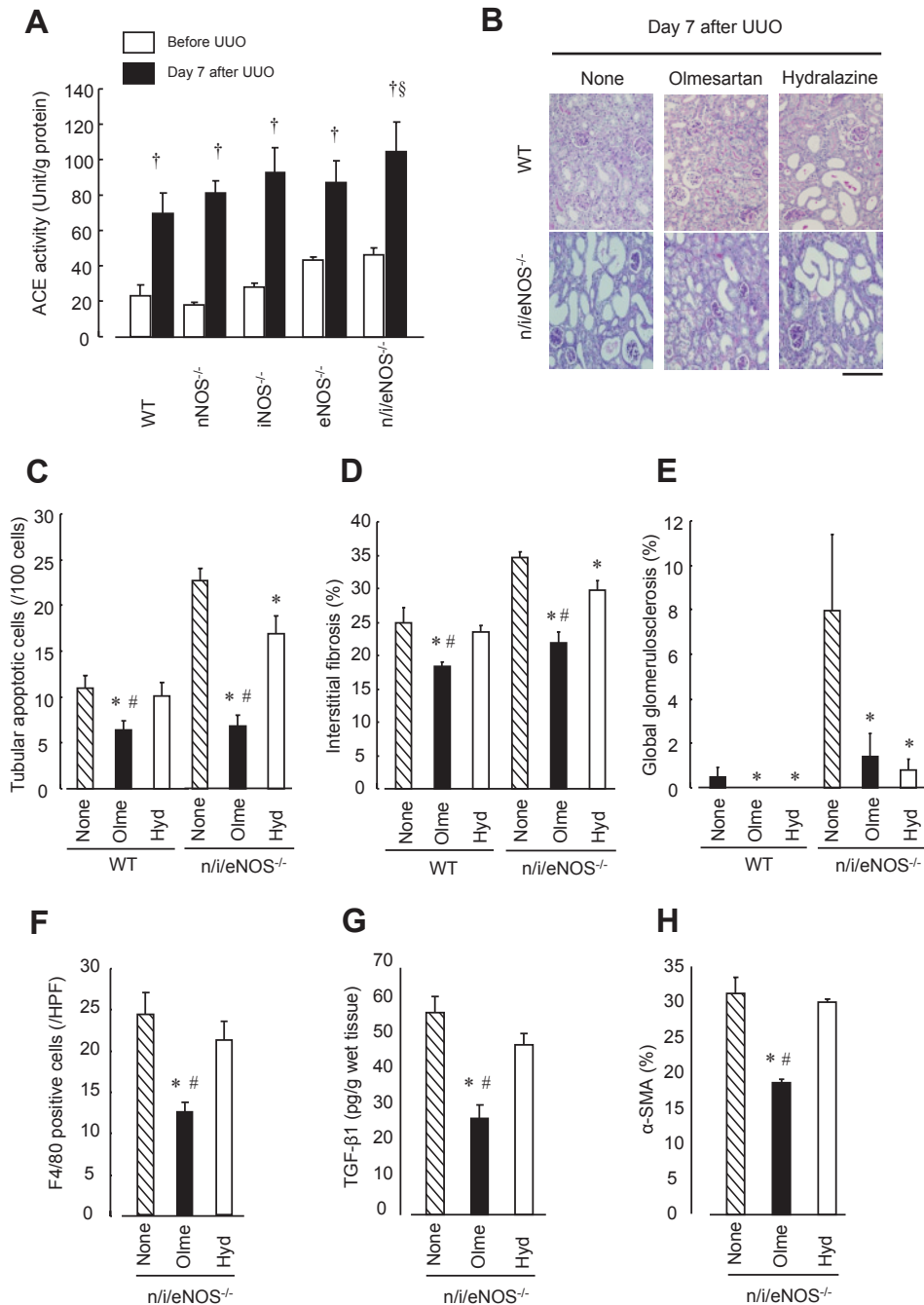


Fig. 5. Angiotensin-converting enzyme (ACE) activity and the effects of long-term treatment with the angiotensin II type 1 (AT₁)-receptor antagonist olmesartan or anti-hypertensive drug hydralazine for 14 days. **A:** ACE activity in the WT, singly NOS $^{-/-}$, and triply NOS $^{-/-}$ mice before and on day 7 after UUU (n = 4–5). [†]*P* < 0.05 vs. before UUU, [§]*P* < 0.05 vs. WT. **B:** PAS staining in the obstructed kidney of the n/i/eNOS $^{-/-}$ mice that received either no treatment, the olmesartan treatment, or the hydralazine treatment. The scale bar represents 100 μ m. **C:** The number of renal tubular apoptotic cells in the obstructed kidney of the n/i/eNOS $^{-/-}$ mice that received either no treatment, the olmesartan treatment, or the hydralazine treatment on day 7 after UUU (n = 4–9). **D:** Interstitial fibrosis (n = 5–9). **E:** Global glomerulosclerosis (n = 4–5). **F:** The number of F4/80-positive cells (n = 4–9). **G:** TGF- β 1 protein levels (each n = 5). **H:** α -SMA-immunoreactive area (n = 4–9). **P* < 0.05 vs. none, #*P* < 0.05 vs. hydralazine.

AT₁-receptor blocker olmesartan, but not anti-hypertensive drug hydralazine, mitigates renal lesion formation after UOU in mice lacking all NOSs

We finally investigated the molecular mechanism(s) for the accelerated renal lesion formation after UOU in the *n/i/eNOS^{-/-}* mice. Renal ACE activity and angiotensin II levels on day 7 after UOU was significantly higher in the *n/i/eNOS^{-/-}* mice than in the WT mice (Fig. 5A). From these results, we further examined our hypothesis that the AT₁-receptor pathway is involved in the exacerbated renal architecture after UOU in the *n/i/eNOS^{-/-}* mice. To this end, we used the AT₁-receptor blocker olmesartan and the anti-hypertensive drug hydralazine (Fig. 5B). Blood pressure (mmHg) was significantly higher in the *n/i/eNOS^{-/-}* mice (111.0 ± 2.3) than in the WT mice (90.8 ± 2.7), and long-term treatment with either olmesartan (100.3 ± 1.1) or hydralazine (103.6 ± 3.4) for 14 days significantly reduced the blood pressure levels of the *n/i/eNOS^{-/-}* mice to a similar extent ($n = 6 - 8$, each $P < 0.05$). The long-term treatment with olmesartan significantly and markedly ameliorated the UOU-induced increases in renal tubular apoptosis (Fig. 5C), interstitial fibrosis (Fig. 5D), and global glomerulosclerosis (Fig. 5E) in the obstructed kidney of the WT and *n/i/eNOS^{-/-}* mice. The inhibitory effects of olmesartan on the UOU-induced increases in renal tubular apoptosis and interstitial fibrosis were greater in the *n/i/eNOS^{-/-}* mice than in the WT mice. The long-term treatment with olmesartan also significantly and markedly alleviated the UOU-induced increases in the number of F4/80-positive macrophages (Fig. 5F), TGF- β 1 levels (Fig. 5G), and α -SMA-positive area (Fig. 5H) in the obstructed kidney of the *n/i/eNOS^{-/-}* mice. Although the long-term treatment with hydralazine significantly inhibited the UOU-induced increases in renal tubular apoptosis (Fig. 5C), interstitial fibrosis (Fig. 5D), and global glomerulosclerosis (Fig. 5E) in the obstructed kidney of the *n/i/eNOS^{-/-}* mice as in the case with olmesartan, the inhibitory effects of hydralazine on renal tubular apoptosis (Fig. 5C) and interstitial fibrosis (Fig. 5D) were significantly less than those of olmesartan. In addition, no significant effect of hydralazine was noted in terms of the number of F4/80-positive macrophages (Fig. 5F), the TGF- β 1 levels (Fig. 5G), or the α -SMA-positive area (Fig. 5H) in the *n/i/eNOS^{-/-}* genotype.

On days 0 and 7 after UOU, renal NOx levels were markedly reduced in the *n/i/eNOS^{-/-}* mice as compared with the WT mice (Fig. 6A). The long-term treatment with olmesartan tended to increase renal NOx levels in both the WT and *n/i/eNOS^{-/-}* mice; however, it did not reach statistically significant difference. Renal angiotensin II levels were significantly higher in the *n/i/eNOS^{-/-}* mice than in the WT mice on days 0 and 7

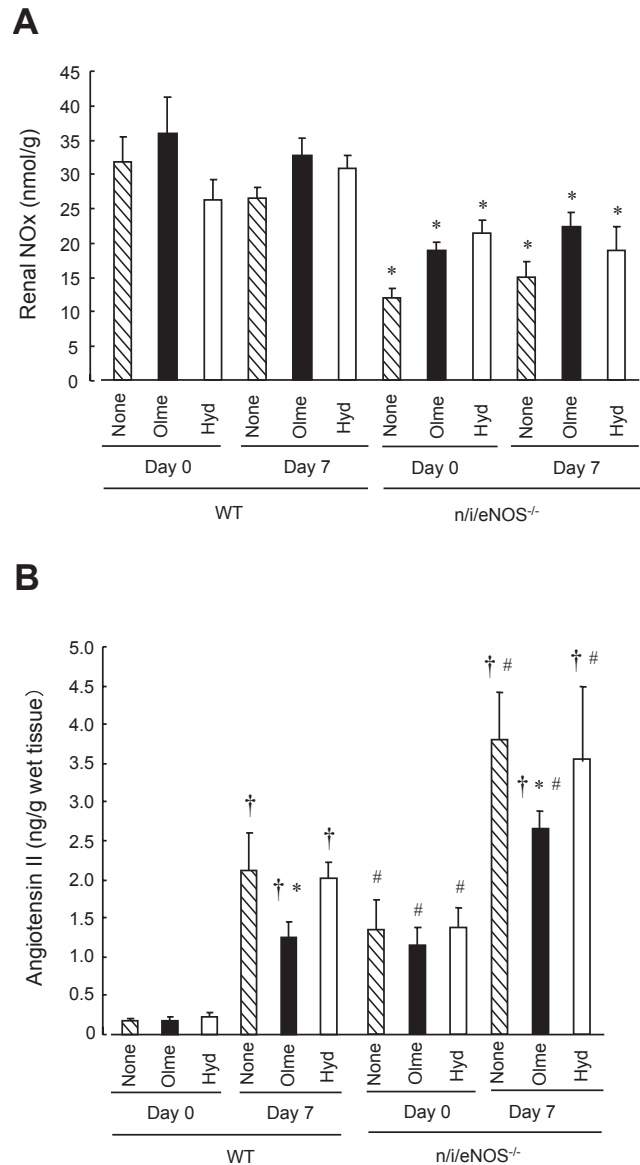


Fig. 6. Renal NOx and angiotensin II levels and the effects of long-term treatment with the AT₁-receptor antagonist olmesartan or anti-hypertensive drug hydralazine for 14 days. A: Renal NOx levels ($n = 5 - 6$). * $P < 0.05$ vs. WT. B: Renal angiotensin II levels ($n = 5 - 6$). # $P < 0.05$ vs. WT, * $P < 0.05$ vs. none, † $P < 0.05$ vs. day 0.

after UOU, and as compared on day 0, renal angiotensin II levels were significantly increased on day 7 after UOU in both the WT and *n/i/eNOS^{-/-}* mice (Fig. 6B). The long-term treatment with olmesartan significantly reduced the increase in renal angiotensin II levels on day 7 after UOU in the two genotypes.

Discussion

The major novel findings of the present study were that the genetic deletion of the entire NOS system re-

sulted in a remarkable exacerbation of renal lesion formation following UUO in mice and that long-term pharmacological blockade of the AT₁ receptor reversed those renal structural changes. These results provide direct evidence for the important role of NO derived from all NOSs in suppressing pathological renal remodeling.

Role of NO derived from all NOSs in renal lesion formation after UUO

Previous studies reported that the eNOS^{-/-} mice exhibit exacerbated renal interstitial fibrosis (14) and global glomerulosclerosis (33) and that the iNOS^{-/-} mice show worsened renal tubular apoptosis (11) and interstitial fibrosis (15, 16). We confirmed those findings in the present study. Although we examined the role of nNOS by using the nNOS^{-/-} mice, there was no significant difference in the extent of renal lesion formation between the WT and nNOS^{-/-} mice. Thus, it is likely that NO derived from eNOS and iNOS, but not from nNOS, plays a role in the UUO-induced renal lesion formation. Notably, the triply NOS^{-/-} mice exhibited the most accelerated renal lesion formation after UUO. Furthermore, NO supplementation by long-term treatment with the NO donor ISDN inhibited the UUO-induced renal lesion formation in the triply NOS^{-/-} mice. Thus, it is possible that NO derived from all NOSs plays a critical renoprotective role in renal lesion formation. Slight but significant increases in renal tubular apoptosis and global glomerulosclerosis were already recognized in the triply NOS^{-/-} mice before UUO, suggesting a possibility that the progression of UUO-induced renal injury in the triply NOS^{-/-} mice might merely depend on renal injury and/or dysfunction at baseline. However, because the marked progression of UUO-induced renal injury was noted in the triply NOS^{-/-} mice but not in the WT mice, and because no renal interstitial fibrosis was observed in the triply NOS^{-/-} mice at baseline, this possibility would be unlikely.

Mechanisms for renal remodeling after UUO in mice lacking all NOSs

The inflammatory reaction plays a pivotal role in the pathogenesis of renal diseases. In the present study, infiltration of inflammatory F4/80-positive macrophages was significantly enhanced in the obstructed kidney of the triply NOS^{-/-} mice, suggesting the involvement of inflammation in renal remodeling after UUO in the genotype. Renal NOx levels were reduced in the triply NOS^{-/-} mice. Since NO exerts an anti-inflammatory effect (1), it is possible that the NO deficiency plays a role in the infiltration of inflammatory cells. Renal angiotensin II levels were enhanced in the obstructed kidney of the triply NOS^{-/-} mice. Because angiotensin II stimulates an

inflammatory reaction (34), it is likely that angiotensin II also plays a role in the inflammatory cell infiltration.

Renal interstitial fibrosis is the final common pathway of a variety of progressive injuries. TGF- β plays a pivotal role in chronic inflammatory changes of the interstitium and accumulation of extracellular matrix during renal fibrogenesis. In this study, increased renal TGF- β levels were noted in the obstructed kidney after UUO in the triply NOS^{-/-} mice, and the renal TGF- β levels were significantly related to the extent of renal interstitial fibrosis. Thus, it is likely that up-regulation of renal TGF- β expression is also involved in the UUO-induced renal remodeling in the triply NOS^{-/-} mice. Consistent with our findings, a previous study reported that targeted disruption of TGF- β 1/Smad3 signaling protects against renal interstitial fibrosis induced by UUO (35).

TGF- β initiates the transition of renal tubular epithelial cells to myofibroblasts, the cellular source of extracellular matrix deposition (i.e., EMT), leading ultimately to irreversible renal failure. The triply NOS^{-/-} mice exhibited a marked increase in α -SMA, a marker of mesenchymal myofibroblasts, in the obstructed kidney, and there was a significant relationship between the renal α -SMA levels and the extent of renal interstitial fibrosis, thus suggesting the involvement of the induction of EMT in the UUO-induced renal lesion formation of the triply NOS^{-/-} mice.

Involvement of AT₁ receptor pathway in renal remodeling after UUO in mice lacking all NOSs

Renal ACE activity and angiotensin II levels after UUO were higher in the triply NOS^{-/-} mice than in the WT mice, suggesting that the renal renin-angiotensin system is activated in the obstructed kidneys of the triply NOS^{-/-} mice. Based on that evidence, we further examined the molecular mechanism(s) for renal remodeling after UUO in the triply NOS^{-/-} mice. The long-term treatment with the AT₁-receptor blocker olmesartan markedly diminished the UUO-induced renal lesion formation in the triply NOS^{-/-} mice, along with the reduction in renal angiotensin II levels. The plasma concentration of olmesartan achieved by the olmesartan treatment that we used in this study has been shown to inhibit the binding of the AT₁ receptor almost completely without affecting the AT₂ receptor (36), indicating that olmesartan antagonizes the AT₁ receptor both selectively and potently under our experimental conditions. It is thus evident that the AT₁-receptor pathway plays a pivotal role in pathological renal remodeling after UUO in the triply NOS^{-/-} genotype.

Although the anti-hypertensive drug hydralazine had an equi-hypotensive property, the inhibitory effects of hydralazine on renal lesion formation after UUO were significantly less than those of olmesartan, and no favor-

able effect of hydralazine on macrophage infiltration, TGF- β , or α -SMA levels was noted. Thus, it is conceivable that the blockade of the AT₁ receptor, rather than the lowering of blood pressure, is involved in the beneficial effects of olmesartan on renal lesion formation after UUO in the triply NOS^{-/-} genotype. The beneficial effects of olmesartan were associated with the reduction in enhanced macrophage infiltration, TGF- β , and α -SMA levels. These results suggest that olmesartan elicits renoprotective effects through inhibitions of the inflammation, TGF- β 1, and EMT.

Clinical implications

Several lines of evidence suggest the association of defective NO production with renal disorders in humans (1). First, it has been reported that urinary NO_x excretion, a marker of NO production derived from all three types of NOSs, are reduced in patients with CKD and ESRD on both peritoneal dialysis and hemodialysis (37–39). Secondly, it has been shown that whole body NO production (as assessed by giving an intravenous infusion of [¹⁵N₂]-arginine and measuring isotopic plasma enrichment of [¹⁵N]-citrulline) is decreased in patients with CKD (40, 41). Finally, it has been indicated that plasma levels of asymmetric dimethylarginine (ADMA), an endogenous NOS inhibitor, are elevated in patients with end-stage chronic renal failure (42). These results may imply the clinical significance of the present findings with the triply NOSs genetic model.

In conclusion, we were able to prove that the complete disruption of all NOS genes causes markedly accelerated renal lesion formation in response to UUO in mice in vivo through the AT₁-receptor pathway, demonstrating the critical renoprotective role of all NOSs-derived NO against pathological renal remodeling. The inflammatory reaction, up-regulation of TGF- β , and induction of EMT appear to be involved in the UUO-induced renal lesion formation. The present findings should contribute to a better understanding of the role of the endogenous NO/NOS system in renal pathophysiology.

Acknowledgments

This work was supported in part by Grants-in-Aid for Young Scientists (B) (20790605) and Grants-in-Aid for Scientific Research (20390074) from the Japan Society for the Promotion of Science, Tokyo, Japan and by grants from the Novartis Foundation for the Promotion of Science, Tokyo, Japan, and the Japan Heart Foundation Grant for Research on Arteriosclerosis Update, Tokyo, Japan.

References

- 1 Baylis C. Nitric oxide deficiency in chronic kidney disease. *Am J Physiol Renal Physiol.* 2008;294:F1–F9.
- 2 Mount PF, Power DA. Nitric oxide in the kidney: functions and regulation of synthesis. *Acta Physiol (Oxf).* 2006;187:433–446.
- 3 Higashi Y, Noma K, Yoshizumi M, Kihara Y. Endothelial function and oxidative stress in cardiovascular diseases. *Circ J.* 2009;73:411–418.
- 4 Brecht DS, Snyder SH. Nitric oxide: a physiological messenger molecule. *Annu Rev Biochem.* 1994;63:175–195.
- 5 Furchgott RF. The role of endothelium in the responses of vascular smooth muscle to drugs. *Annu Rev Pharmacol Toxicol.* 1984;24:175–197.
- 6 Ignarro LJ. Biosynthesis and metabolism of endothelium-derived nitric oxide. *Annu Rev Pharmacol Toxicol.* 1990;30:535–560.
- 7 Moncada S, Palmer RMJ, Higgs EA. Nitric oxide: physiology, pathophysiology, and pharmacology. *Pharmacol Rev.* 1991;43:109–142.
- 8 Murad F. What are the molecular mechanisms for the antiproliferative effects of nitric oxide and cGMP in vascular smooth muscle? *Circulation.* 1997;95:1101–1103.
- 9 Shimokawa H. Primary endothelial dysfunction: atherosclerosis. *J Mol Cell Cardiol.* 1999;31:23–37.
- 10 Tsutsui M, Shimokawa H, Otsuji Y, Ueta Y, Sasaguri Y, Yanagihara N. Nitric oxide synthases and cardiovascular diseases: insights from genetically modified mice. *Circ J.* 2009;73:986–993.
- 11 Miyajima A, Chen J, Poppas DP, Vaughan ED Jr, Felsen D. Role of nitric oxide in renal tubular apoptosis of unilateral ureteral obstruction. *Kidney Int.* 2001;59:1290–1303.
- 12 Morrissey JJ, Ishidoya S, McCracken R, Klahr S. Nitric oxide generation ameliorates the tubulointerstitial fibrosis of obstructive nephropathy. *J Am Soc Nephrol.* 1996;7:2202–2212.
- 13 Kuncio GS, Neilson EG, Haverty T. Mechanisms of tubulointerstitial fibrosis. *Kidney Int.* 1991;39:550–556.
- 14 Chang B, Mathew R, Palmer LS, Valderrama E, Trachtman H. Nitric oxide in obstructive uropathy: role of endothelial nitric oxide synthase. *J Urol.* 2002;168:1801–1804.
- 15 Hochberg D, Johnson CW, Chen J, Cohen D, Stern J, Vaughan ED Jr, et al. Interstitial fibrosis of unilateral ureteral obstruction is exacerbated in kidneys of mice lacking the gene for inducible nitric oxide synthase. *Lab Invest.* 2000;80:1721–1728.
- 16 Huang A, Palmer LS, Hom D, Valderrama E, Trachtman H. The role of nitric oxide in obstructive nephropathy. *J Urol.* 2000;163:1276–1281.
- 17 Morishita T, Tsutsui M, Shimokawa H, Sabanai K, Tasaki H, Suda O, et al. Nephrogenic diabetes insipidus in mice lacking all nitric oxide synthase isoforms. *Proc Natl Acad Sci U S A.* 2005;102:10616–10621.
- 18 Tsutsui M, Shimokawa H, Morishita T, Nakashima Y, Yanagihara N. Development of genetically engineered mice lacking all three nitric oxide synthases. *J Pharmacol Sci.* 2006;102:147–154.
- 19 el-Dahr SS, Gee J, Dipp S, Hanss BG, Vari RC, Chao J. Upregulation of renin-angiotensin system and downregulation of kallikrein in obstructive nephropathy. *Am J Physiol.* 1993;264:F874–F881.
- 20 Yoo KH, Norwood VF, el-Dahr SS, Yosipiv I, Chevalier RL. Regulation of angiotensin II AT₁ and AT₂ receptors in neonatal ureteral obstruction. *Am J Physiol.* 1997;273:R503–R509.
- 21 Ishidoya S, Morrissey J, McCracken R, Reyes A, Klahr S. Angiotensin II receptor antagonist ameliorates renal tubulointerstitial fibrosis caused by unilateral ureteral obstruction. *Kidney Int.* 1995;47:1285–1294.

- 22 El Chaar M, Chen J, Seshan SV, Jha S, Richardson I, Ledbetter SR, et al. Effect of combination therapy with enalapril and the TGF-beta antagonist 1D11 in unilateral ureteral obstruction. *Am J Physiol Renal Physiol.* 2007;292:F1291–F1301.
- 23 Fern RJ, Yesko CM, Thornhill BA, Kim HS, Smithies O, Chevalier RL. Reduced angiotensinogen expression attenuates renal interstitial fibrosis in obstructive nephropathy in mice. *J Clin Invest.* 1999;103:39–46.
- 24 Satoh M, Kashihara N, Yamasaki Y, Maruyama K, Okamoto K, Maeshima Y, et al. Renal interstitial fibrosis is reduced in angiotensin II type 1a receptor-deficient mice. *J Am Soc Nephrol.* 2001;12:317–325.
- 25 Suda O, Tsutsui M, Morishita T, Tanimoto A, Horiuchi M, Tasaki H, et al. Long-term treatment with N(omega)-nitro-L-arginine methyl ester causes arteriosclerotic coronary lesions in endothelial nitric oxide synthase-deficient mice. *Circulation.* 2002;106:1729–1735.
- 26 Guo G, Morrissey J, McCracken R, Tolley T, Liapis H, Klahr S. Contributions of angiotensin II and tumor necrosis factor-alpha to the development of renal fibrosis. *Am J Physiol Renal Physiol.* 2001;280:F777–F785.
- 27 Kaneto H, Morrissey J, McCracken R, Reyes A, Klahr S. Enalapril reduces collagen type IV synthesis and expansion of the interstitium in the obstructed rat kidney. *Kidney Int.* 1994;45:1637–1647.
- 28 Yabuki A, Maeda M, Matsumoto M, Kamimura R, Masuyama T, Suzuki S. SAMP1/Sku as a murine model for tubulointerstitial nephritis: a study using unilateral ureteral obstruction. *Exp Anim.* 2005;54:53–60.
- 29 Inoue T, Plieth D, Venkov CD, Xu C, Neilson EG. Antibodies against macrophages that overlap in specificity with fibroblasts. *Kidney Int.* 2005;67:2488–2493.
- 30 Nakata S, Tsutsui M, Shimokawa H, Suda O, Morishita T, Shibata K, et al. Spontaneous myocardial infarction in mice lacking all nitric oxide synthase isoforms. *Circulation.* 2008;117:2211–2223.
- 31 Prathapasinghe GA, Siow YL, Xu Z, O K. Inhibition of cystathionine-beta-synthase activity during renal ischemia-reperfusion: role of pH and nitric oxide. *Am J Physiol Renal Physiol.* 2008;295:F912–F922.
- 32 Wimalawansa SJ, De Marco G, Gangula P, Yallampalli C. Nitric oxide donor alleviates ovariectomy-induced bone loss. *Bone.* 1996;18:301–304.
- 33 Nakayama T, Sato W, Kosugi T, Zhang L, Campbell-Thompson M, Yoshimura A, et al. Endothelial injury due to eNOS deficiency accelerates the progression of chronic renal disease in the mouse. *Am J Physiol Renal Physiol.* 2009;296:F317–F327.
- 34 Bader M. Tissue renin-angiotensin-aldosterone systems: targets for pharmacological therapy. *Annu Rev Pharmacol Toxicol.* 2010;50:439–465.
- 35 Sato M, Muragaki Y, Saika S, Roberts AB, Ooshima A. Targeted disruption of TGF-beta1/Smad3 signaling protects against renal tubulointerstitial fibrosis induced by unilateral ureteral obstruction. *J Clin Invest.* 2003;112:1486–1494.
- 36 Nakamura H, Inoue T, Arakawa N, Shimizu Y, Yoshigae Y, Fujimori I, et al. Pharmacological and pharmacokinetic study of olmesartan medoxomil in animal diabetic retinopathy models. *Eur J Pharmacol.* 2005;512:239–246.
- 37 Schmidt RJ, Baylis C. Total nitric oxide production is low in patients with chronic renal disease. *Kidney Int.* 2000;58:1261–1266.
- 38 Schmidt RJ, Domico J, Samsell LS, Yokota S, Tracy TS, Sorkin MI, et al. Indices of activity of the nitric oxide system in hemodialysis patients. *Am J Kidney Dis.* 1999;34:228–234.
- 39 Schmidt RJ, Yokota S, Tracy TS, Sorkin MI, Baylis C. Nitric oxide production is low in end-stage renal disease patients on peritoneal dialysis. *Am J Physiol.* 1999;276:F794–F797.
- 40 Lau T, Owen W, Yu YM, Noviski N, Lyons J, Zurakowski D, et al. Arginine, citrulline, and nitric oxide metabolism in end-stage renal disease patients. *J Clin Invest.* 2000;105:1217–1225.
- 41 Wever R, Boer P, Hijmering M, Stroes E, Verhaar M, Kastelein J, et al. Nitric oxide production is reduced in patients with chronic renal failure. *Arterioscler Thromb Vasc Biol.* 1999;19:1168–1172.
- 42 Vallance P, Leone A, Calver A, Collier J, Moncada S. Accumulation of an endogenous inhibitor of nitric oxide synthesis in chronic renal failure. *Lancet.* 1992;339:572–575.